

CHAPTER 41
 THE DYNAMICS OF A SUBMERGED MOORED SPHERE
 IN OSCILLATORY WAVES

Donald R. F. Harleman
 Associate Professor of Hydraulics
 Hydrodynamics Laboratory
 Massachusetts Institute of Technology

and

William C. Shapiro
 Assistant Professor of Civil Engineering
 The Cooper Union

The results of an analytical and experimental investigation into the dynamics of a buoyant sphere moored by a single line in shallow water waves are presented. The sphere motion and the mooring line forces are related to the sphere diameter, weight, submergence and the wave frequency, height and water depth. Analytically, the phenomenon is approached as a forced vibration problem. The sphere and its mooring line acts as a spring-mass system driven by the oscillating wave force. The relevant dimensionless parameters are the ratio between the natural frequency of the moored sphere and the wave frequency and the ratio between the dynamic mooring force due to a given wave and the force on the sphere held stationary in the same wave. Experimental values of the frequency and force ratios obtained from tests made at the Massachusetts Institute of Technology Hydrodynamics Laboratory over a range of sphere and wave characteristics are in essential agreement with the analytically determined values. The investigation was supported by the Humble Oil and Refining Company of Houston, Texas.

ANALYTICAL DEVELOPMENT

WAVE FORCE ON A STATIONARY SPHERE

The forces on objects submerged in water waves result from the velocities and accelerations of the water particles comprising the waves. For waves having a steepness H/L less than 0.03 the particle kinematics are given by the Airy equations. The equations for the horizontal and vertical components of particle velocity and acceleration expressed in the notation of Figure 1 are

$$u = \frac{\sigma H}{2} \left(\frac{\cosh kS}{\sinh kd} \right) \sin \sigma t = u_m \sin \sigma t \quad (1)$$

$$v = \frac{\sigma H}{2} \left(\frac{\sinh kS}{\sinh kd} \right) \cos \sigma t = v_m \cos \sigma t \quad (2)$$

$$\frac{du}{dt} = \frac{\sigma^2 H}{2} \left(\frac{\cosh kS}{\sinh kd} \right) \cos \sigma t = \left(\frac{du}{dt} \right)_m \cos \sigma t \quad (3)$$

$$\frac{dv}{dt} = - \frac{\sigma^2 H}{2} \left(\frac{\sinh kS}{\sinh kd} \right) \sin \sigma t = - \left(\frac{dv}{dt} \right)_m \sin \sigma t \quad (4)$$

THE DYNAMICS OF A SUBMERGED MOORED SPHERE IN OSCILLATORY WAVES

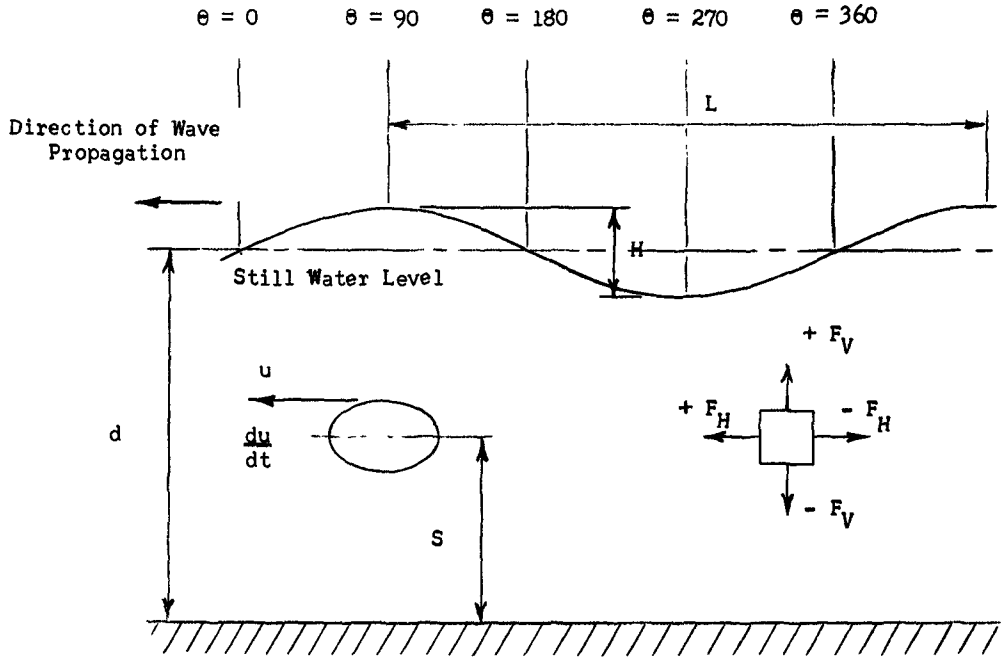


Fig. 1. Definition sketch for wave motion.

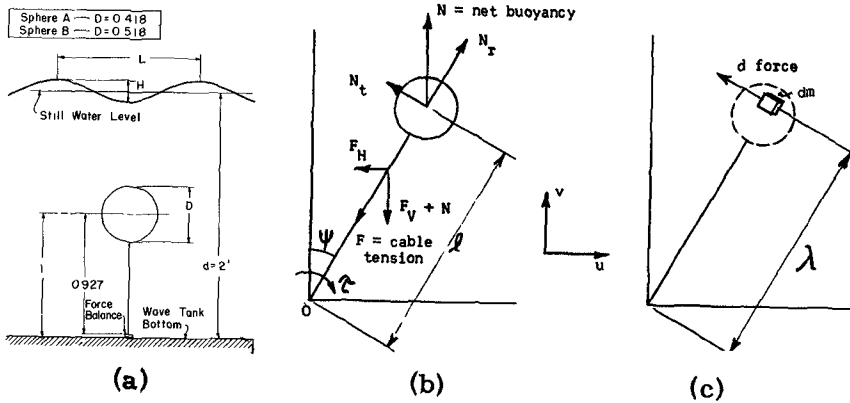


Fig. 2. Definition sketch for moored sphere.

COASTAL ENGINEERING

The speed of wave propagation or celerity is

$$\text{celerity} = \frac{L}{T} = \sqrt{\frac{g}{K} \tanh kd} \quad (5)$$

In the absence of viscosity, the force exerted on an object in an unsteady flow field may be determined from classical hydrodynamic theory. The pressure gradient in the horizontal direction resulting from the local acceleration (convective acceleration terms neglected) is given by the equation of motion.

$$-\frac{dp}{dx} = \rho \frac{du}{dt} \quad (6)$$

By integration, the force on an object due to the pressure gradient becomes

$$F_H(\text{pressure grad}) = -\frac{dp}{dx}(\text{Vol.}) = \rho(\text{Vol.}) \frac{du}{dt} = M \frac{du}{dt} \quad (7)$$

where M is the mass of the displaced fluid.

In addition to the pressure gradient force there is a force due to virtual mass which exists whenever there is relative acceleration between a fluid and an immersed body. The virtual mass force can be expressed

$$F_H(\text{virtual mass}) = K \rho(\text{Vol.}) \frac{du}{dt} = KM \frac{du}{dt} \quad (8)$$

where K is the added mass constant. Addition of equations (7) and (8) gives the total acceleration or inertia force.

$$F_{HI} = (1 + K) M \frac{du}{dt} = C_M \rho(\text{Vol.}) \frac{du}{dt} \quad (9)$$

In equation (9) C_M , the coefficient of mass replaces the term $(1+K)$. The added mass constant K has been determined analytically for a sphere to be 0.5. C_M for a sphere in frictionless flow is therefore 1.5.

The force on an object in steady viscous flow arises from surface shear, pressure gradients and wake formation. The hydrodynamic drag is expressed

$$F_{HD} = C_D \frac{\rho}{2} (\text{Area}) |u| u \quad (10)$$

To obtain the wave force on a submerged stationary object the steady state drag force given by equation (10) is added to the potential flow inertia force given by equation (9)

$$F_{HO} = F_{HI} + F_{HD} = C_M \rho(\text{Vol.}) \frac{du}{dt} + C_D \frac{\rho}{2} (\text{Area}) |u| u \quad (11)$$

THE DYNAMICS OF A SUBMERGED MOORED SPHERE IN OSCILLATORY WAVES

Substitution of the wave particle velocity and acceleration expressions into equation (11) yields

$$F_{HO} = C_M \rho (\text{Vol.}) \left[\frac{du}{dt} \right]_m \cos \sigma t + C_D \rho / 2 (\text{Area}) u_m^2 |\sin \sigma t| \sin \sigma t \quad (12)$$

Assuming C_M and C_D to be constant over a wave cycle, equation (12) may be rewritten

$$F_{HO} = F_{HIm} \cos \sigma t + F_{HDm} |\sin \sigma t| \sin \sigma t \quad (13)$$

where

$$F_{HIm} = C_M \rho (\text{Vol.}) \left[\frac{du}{dt} \right]_m \quad (14)$$

$$F_{HDm} = C_D \rho / 2 (\text{Area}) u_m^2 \quad (15)$$

Using the Stokes solution of a sphere oscillating in a viscous fluid at low Reynolds numbers and dimensional analysis, Keulegan and Carpenter (1958) successfully correlated experimentally determined inertia and drag coefficients with a period parameter $u_m T/D$. The parameter $u_m T/D$ is directly related to the ratio of the maximum wave drag force component to the maximum inertia component. For a sphere, equations (14) and (15) with the use of equations (1) and (3) give

$$\frac{F_{HIm}}{F_{HDm}} = \frac{8}{3} \pi \frac{C_M}{C_D} \left[1 / \frac{u_m T}{D} \right] \quad (16)$$

From equation (16) a low value of period parameter signifies a predominant inertia force while a high value signifies a predominant drag force. Using a cylinder in the sinusoidal horizontal current under the node of a standing wave, Keulegan and Carpenter found the experimentally determined inertia coefficient equal to the potential flow value for low period parameters and the drag coefficient equal to the steady state value for high period parameter. Between these two extreme cases a point of maximum deviation of both the inertia and drag coefficients from their potential flow and steady state values respectively was found at a period parameter of 15.

Keulegan and Carpenter's results indicate that equation (12) may be used to determine the wave force on a submerged object provided the inertia and drag coefficients are known as functions of the period parameter. In the special case where the inertia force predominates and the drag force is small (low period parameters) the potential flow value of the inertia coefficient may be used. In the special case where drag force predominates and the inertia force is small (high period parameter) the steady state value of the drag coefficient may be used.

COASTAL ENGINEERING

The reasoning outlined above is supported by the results of Harleman and Shapiro (1955) in their tests on single vertical cylinders in steep waves. In their analysis they used essentially the formulation of equation (12) to construct the total wave force history with the potential flow C_M and the steady state C_D . Their analytical results were in agreement with experiment for the cases of predominant inertia and predominant drag, but were not in agreement for the region of approximately equal inertia and drag. The greatest discrepancy between analysis and experiment occurred near $u_m T/D = 15$.

The relationship between the period parameter and the wave and object characteristics is found by substituting from equation (1) for u_m .

$$\frac{u_m T}{D} = \frac{\pi H}{D} \frac{\cosh kS}{\sinh kd} \quad (17)$$

The experiments in this study were conducted using waves of steepness: $H/L = 0.02$. This small steepness was chosen to simplify the analysis of the problem through the use of the Airy equations for wave kinematics. In addition, wave and sphere dimensions were selected to yield low period parameters; that is, a condition of predominant inertia force. The subsequent analysis will be seen to depend upon this condition. The wave and sphere characteristics used in this study are shown in Table I and Figure 2a.

The preceding discussion of wave forces on rigidly restrained bodies has been concerned with the horizontal wave force component. However, all the foregoing applies to the vertical component as well. The following are the relevant equations for the vertical component.

$$F_{VI} = (1+k) \rho (\text{Vol.}) dv/dt = C_M \rho (\text{Vol.}) dv/dt \quad (18)$$

$$F_{VD} = C_D \rho / 2 (\text{Area}) |v| v \quad (19)$$

$$F_{VO} = F_{VI} + F_{VD} = C_M \rho (\text{Vol.}) dv/dt + C_D \rho / 2 (\text{Area}) |v| v \quad (20)$$

$$F_{VO} = F_{VI_m} \sin \sigma t + F_{VD_m} |\cos \sigma t| \cos \sigma t \quad (21)$$

$$F_{VI_m} = C_M \rho (\text{Vol.}) [dv/dt]_m \quad (22)$$

$$F_{VD_m} = C_D \rho / 2 (\text{Area}) v_m^2 \quad (23)$$

ANALYSIS OF MOORED OSCILLATING SPHERE

Figure 2 is the definition sketch for the moored sphere analysis. It is assumed in the analysis that the mooring line remains straight and under tension at all times and that the sphere motion remains in the plane defined by the wave particle orbits. These assumptions permit the position of the sphere to be uniquely defined by the mooring line angle, ψ alone. Thus the sphere and mooring line constitute a single degree of

THE DYNAMICS OF A SUBMERGED MOORED SPHERE IN OSCILLATORY WAVES

freedom oscillating system.

Referring to Figure 2c, Newton's second law is written in the tangential direction for the element of mass dm .

$$d \text{ Force} = dm \ddot{\psi} \lambda$$

where $\ddot{\psi}$ is the angular acceleration. Multiplying both sides of the equation by λ gives

$$d \text{ Torque} = \lambda^2 dm \ddot{\psi}$$

Integration over the volume of the sphere yields

$$T = I \ddot{\psi} \tag{24}$$

where I is the moment of inertia of the sphere about point O since

$$\int_{\text{VOL.}} \lambda^2 dm = I$$

Equation (24) is the standard form of Newton's second law for rotating bodies. The torque, T , is the summation of the torques due to all the forces acting on the sphere. The first of these is the spring torque. Assuming that the mooring line angle remains small, so that $\sin \psi \approx \psi$, the spring torque is

$$\begin{aligned} \text{Spring torque} &= -N_t \ell = -N \ell \sin \psi \\ &\approx - \left[\frac{\pi D^3}{6} \rho g - mg \right] \ell \psi \end{aligned} \tag{25}$$

The pressure gradient torque depends upon the fluid acceleration and is derived from equation (7). Here the flow field is specified in terms of horizontal and vertical components. To find the total pressure gradient torque it is necessary to take the sum of the projections in the tangential direction of the horizontal and vertical pressure gradient force components. Assuming again that the mooring line angle remains small

$$\begin{aligned} \text{Pressure grad. torque} &= \frac{\pi D^3}{6} \rho \left[\frac{du}{dt} \cos \psi - \frac{dv}{dt} \sin \psi \right] \ell \\ &\approx \frac{\pi D^3}{6} \rho \left[\frac{du}{dt} - \frac{dv}{dt} \psi \right] \ell \end{aligned} \tag{26}$$

The virtual mass torque depends upon the relative acceleration between the fluid and the sphere. In view of equation (8) the virtual mass effect is assumed due to a sphere of fluid the same size as the actual sphere but having a mass equal to K times the mass of the fluid. Following the method used in deriving equation (24) and using equation (8), the virtual mass torque may be written

COASTAL ENGINEERING

$$\begin{aligned} \text{Virtual mass torque} &= -I'\ddot{\psi} + \frac{K\pi D^3}{6} \rho \left[\frac{du}{dt} \cos\psi - \frac{dv}{dt} \sin\psi \right] l \\ &\approx -I'\ddot{\psi} + \frac{K\pi D^3}{6} \rho \left[\frac{du}{dt} - \frac{dv}{dt} \psi \right] l \end{aligned} \quad (27)$$

where I' is the moment of inertia of the fluid sphere about point O and the mooring line angle is assumed small.

The damping torque depends on the relative velocity between the sphere and the fluid. Assuming, for the present, the damping to be linear and the mooring line angle small, the damping torque may be written

$$\begin{aligned} \text{Damping torque} &= c [-\dot{\psi}l + u \cos\psi - v \sin\psi] l \\ &\approx c [-\dot{\psi}l + u - v\psi] l \end{aligned} \quad (28)$$

The contributing torques given by equations (25) through (28) are added and substituted into equation (24) to give the equation of motion of the oscillating sphere with linear damping

$$\begin{aligned} (I + I')\ddot{\psi} + c\dot{\psi}l^2 + \underbrace{\left[\frac{\pi D^3}{6} \rho g - mg \right]}_{\text{net buoyancy}} + \underbrace{(K+1) \frac{\pi D^3}{6} \rho \frac{dv}{dt}}_{F_{vo}} + cv] l \psi \\ = \underbrace{\left[(K+1) \frac{\pi D^3}{6} \rho \frac{du}{dt} \right]}_{\text{Inertia}} + \underbrace{cu}_{\text{Drag}}] l \end{aligned} \quad (29)$$

Equation (29) has the general form of the differential equation of motion of a single degree of freedom spring-mass system with linear damping. However, in its present form the equation is non-linear.

The physical meaning of the various portions of equation (29) is indicated by brackets. To linearize and simplify the equation the following assumptions are made:

- Assumption 1 The vertical component of the mooring line force is equal to the net buoyancy N . This is valid if the vertical dynamic wave force F_v is small with respect to the net buoyancy.
- Assumption 2 The drag wave force component is small with respect to the inertia wave force component.
- Assumption 3 (previously stated) The mooring line angle, ψ , is small

With assumptions 1 and 2, equation (29) becomes

$$(I + I')\ddot{\psi} + (c l^2)\dot{\psi} + \left(\frac{\pi D^3}{6} \rho g - mg \right) l \psi = C_M \frac{\pi D^3}{6} \rho \frac{du}{dt} l \quad (30)$$

THE DYNAMICS OF A SUBMERGED MOORED SPHERE IN OSCILLATORY WAVES

The preceding assumptions have reduced the equation of motion to the exact form of the differential equation of motion of the single degree of freedom spring-mass system with linear damping and a sinusoidal driving force. The more practical case for the sphere problem involves quadratic damping as given by equation (10). In order to revise the preceding analysis for square law damping it is only necessary to change the damping term in equation (30). The damping torque is now given by

$$\text{Damping torque} = c_2 (\dot{\psi} l)^2 l = c_2 \dot{\psi}^2 \quad (31)$$

where

$$C_2 = c_2 l^3 \quad (32)$$

The differential equation of motion becomes

$$A \ddot{\psi} + C_2 \dot{\psi}^2 + B \psi = F_{H_{om}} l \cos \sigma t \approx F_{H_{Im}} \cos \sigma t \quad (33)$$

where

$$A = I + I', \quad B = \left[\frac{\pi D^3}{6} \rho g - mg \right] l = N l \quad (34)$$

Before treating the solution of equation (33) as written, the special case of free oscillation of the moored submerged sphere without damping will be considered. Setting the driving force and damping terms to zero in equation (33) yields the differential equation of motion for the free oscillation case.

$$A \ddot{\psi} + B \psi = 0 \quad (35)$$

Equation (35) has the solution

$$\psi = \psi_m \cos \sqrt{\frac{B}{A}} \cdot t \quad (36)$$

The motion is sinusoidal with amplitude or maximum angle and frequency

$$f_n = \frac{1}{2\pi} \sqrt{\frac{B}{A}} \quad (37)$$

The frequency given by equation (37) is the undamped natural frequency. From vibration theory the solution to the free oscillation problem with linear damping included is known to be a harmonic oscillation with an exponentially decreasing amplitude and a frequency somewhat less than the undamped natural frequency. For small damping however, the damped natural frequency is equal to the undamped natural frequency for all practical purposes.

In Figure 3 experimentally determined natural frequencies are plotted against sphere weight for the 0.518 ft. sphere. Also shown is the theoretical curve computed for the test conditions from equation (37) using the potential flow added mass coefficient of 0.5. The excellent agreement between theory and experiment shows the neglect of damping in

COASTAL ENGINEERING

the free oscillation case is justified for the conditions of this study.

The non-linear forced oscillation equation of motion with quadratic damping [equation (33)] can be solved as a linear equation by using the technique of Lorentz which was originally devised in 1926 for tidal computations in shallow water (Dronkers and Schonfeld 1955). The dissipation of energy in one wave period by the quadratic resistance term is equated to the dissipation represented by the linear term in equation (29). A similar method has also been used by Jacobsen (1930) in connection with mechanical vibration problems. Under the above conditions the solution of equation (33) is given by

$$\psi = \psi_m \cos(\sigma t - \phi) \quad (38)$$

According to equation (38) the sphere moored in oscillatory waves oscillates sinusoidally at the wave frequency and lags the driving force by a phase shift ϕ . The amplitude of oscillation is a function of the ratio between the wave (driving) frequency and the natural frequency of the system. In dimensionless form the amplitude and phase shift are

$$\frac{\psi_m}{\psi_{om}} = \frac{F_{Hm}}{F_{Hom}} = \frac{1}{\sqrt{2} n_2 (f/f_n)^2} \left[\left\{ \left(1 - \left(\frac{f}{f_n}\right)^2\right)^4 - 4 n_2^2 \left(\frac{f}{f_n}\right)^4 \right\}^{1/2} - \left(1 - \left(\frac{f}{f_n}\right)^2\right)^2 \right]^{1/2} \quad (39)$$

and

$$\tan \phi = \frac{1}{\sqrt{2}} \left[\left\{ 1 + \frac{4 n_2^2 (f/f_n)^4}{(1 - (f/f_n)^2)^4} \right\}^{1/2} - 1 \right]^{1/2} \quad (40)$$

where

$$\psi_{om} = \frac{T_{om}}{B} = \frac{F_{Hom} l}{\left[\frac{\pi D^3}{6} \rho g - mg\right] l} = \frac{F_{Hom}}{N} \quad (41)$$

In view of assumptions 1 and 3, the parameter ψ_{om} represents the mooring line angle which would obtain if the sphere were subjected statically to the horizontal driving force maximum, F_{Hom} . The term ψ_m/ψ_{om} is the multiplication factor between the static deflection of the sphere under the driving force, and the amplitude of the actual sphere motion.

In accordance with assumptions 1 and 3

$$\frac{\psi_m}{\psi_{om}} = \frac{F_{Hm}}{F_{Hom}}$$

where F_{Hm} is the maximum value of the horizontal component of mooring line tension. Therefore equation (39) also describes the variation in the horizontal mooring line tension multiplication factor with

THE DYNAMICS OF A SUBMERGED MOORED SPHERE IN OSCILLATORY WAVES

Table I: CHARACTERISTICS OF EXPERIMENTAL PROGRAM

Test	Wave Height ft.	Wave Length ft.	Period sec.	Freq. cps	Wave Freq. Nat. Freq.	Period Parameter $u_m T/D$
I-2-A	0.10	5.10	1.00	1.000	1.00-3.10	0.24
I-2-B	"	"	"	"	1.02-3.20	0.20
I-4-A	0.20	9.90	1.50	0.667	1.14-1.08	1.10
I-4-B	"	"	"	"	1.14-1.08	0.88
I-6-A	0.29	14.45	2.00	0.500	0.50-1.63	2.42
I-6-B	"	"	"	"	0.50-1.56	1.95
I-7-A	0.33	16.65	2.75	0.445	0.45-1.38	3.24
I-7-B	"	"	"	"	0.44-1.40	2.61

All tests: Water depth = 2 ft., Sphere moored at mid-depth
 Sphere A: Diam. = 0.418 ft.
 Sphere B: Diam. = 0.518 ft.

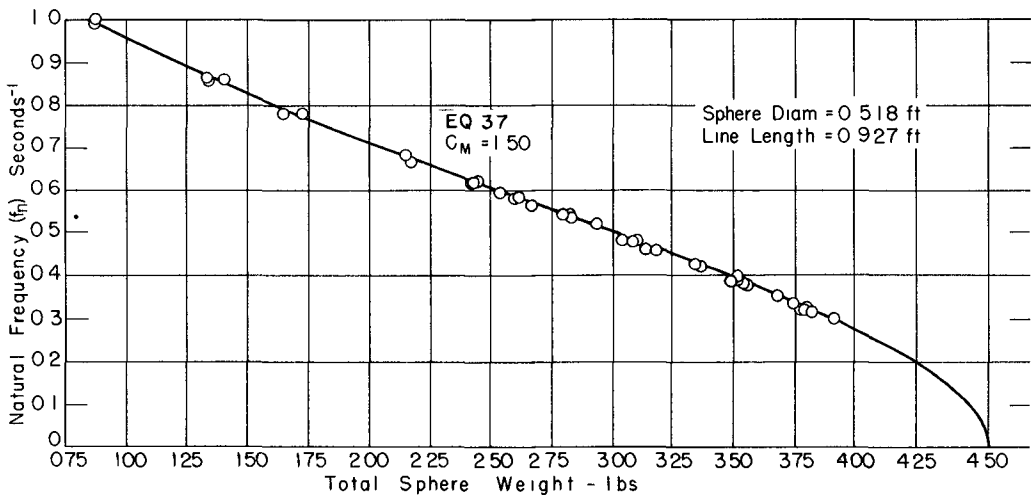


Fig. 3. Variation of natural frequency with weight of sphere.

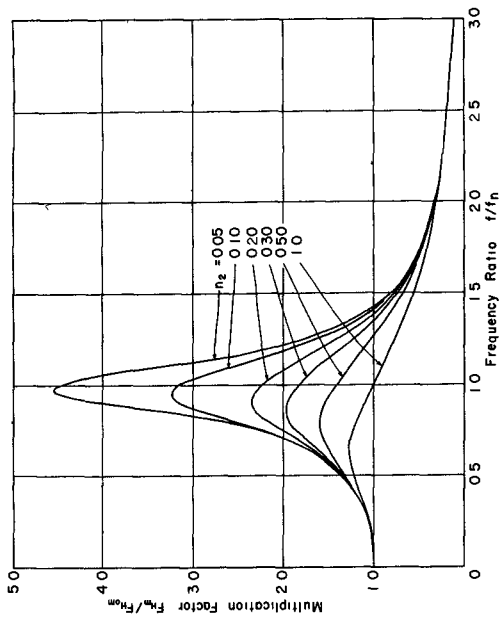


Fig. 4. Horizontal force multiplication factor for quadratic damping.

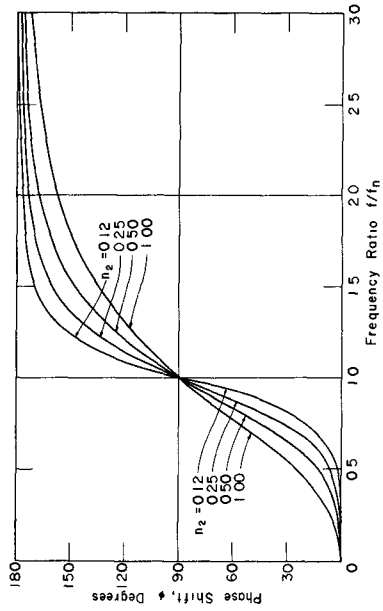


Fig. 5. Horizontal force phase shift for quadratic damping.

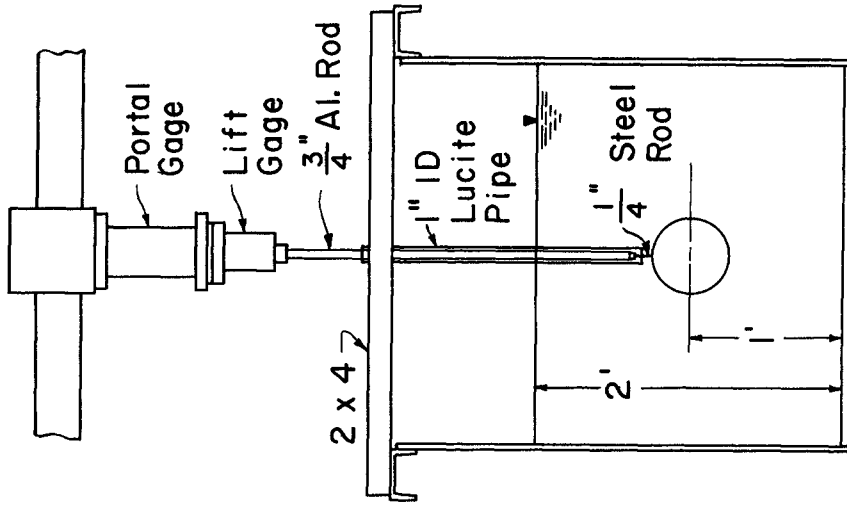


Fig. 6. Rigidly restrained sphere test arrangement.

THE DYNAMICS OF A SUBMERGED MOORED SPHERE IN OSCILLATORY WAVES

frequency ratio.

The damping factor, n_2 , in equations (39) and (40) is

$$n_2 = \frac{2}{3} \frac{C_2 F_{H_{om}} \lambda}{\pi^3 A^2 f_n^2} \quad (43)$$

The constant $c_2 = C_2/\lambda^3$ is found from the drag force equation, equation (10) with the cross sectional area of the sphere inserted

$$F_{HD} = \underbrace{C_D \rho/2 \frac{\pi D^2}{4}}_{c_2} |u|u$$

Therefore

$$n_2 = \frac{1}{12\pi^2} \frac{C_D \rho D^2 \lambda^4 F_{H_{om}}}{A^2 f_n^2} \quad (44)$$

Figure 4 is a plot of the multiplication factor against frequency ratio computed from equation (39) for several values of the parameter n_2 . The phase shift given by equation (40) is plotted in Figure 5. Figures 4 and 5 show the three primary modes of behavior of the oscillating sphere. At very low frequency ratios the horizontal mooring line force component is in phase with and opposed to the driving force. This is the condition of static response because at any point of the cycle the restraining force is exactly equal to the applied force. At frequency ratios near unity, the damping force is in phase with and opposed to the driving force and the horizontal mooring line force achieves large magnitudes dependent upon the amount of damping. This is the condition of resonance. At large frequency ratios, the inertia force is in phase with and opposed to the driving force and the horizontal mooring line force approaches zero. This is the condition of complete dynamic response.

Use of the Analytical Relationships

To summarize the theoretical development, the procedure for determining the maximum mooring line tension in a particular problem will be reviewed. First, the period parameter is computed from equation (17) to determine if the condition of predominant inertia force is satisfied. To satisfy this condition, the period parameter should be less than 5.

Second, the maximum horizontal force on the stationary sphere, $F_{H_{om}}$ is computed. Since the drag component of the total force is small, equation (14), the equation for the maximum inertia component may be used to closely approximate $F_{H_{om}}$.

Third, the natural frequency of the sphere is determined from equation (37) and divided into the wave frequency to give the frequency ratio.

Fourth, the multiplication factor is computed from equation (39) using the n_2 value obtained from equation (44). In this computation C_D is determined from the steady state drag curve using as Reynolds number

COASTAL ENGINEERING

$u_m D/\lambda$). The maximum force on the stationary sphere is multiplied by the multiplication factor to give the maximum horizontal mooring line tension component. The maximum mooring line angle is determined from the relationship.

$$\psi_m = \tan^{-1} \frac{F_{Hm}}{N} \approx \frac{F_{Hm}}{N} \quad (45)$$

The maximum mooring line tension is determined from the relation

$$\text{Maximum Tension} = \sqrt{(F_{Hm})^2 + N^2} \quad (46)$$

EXPERIMENTAL PROGRAM

EXPERIMENTAL EQUIPMENT

The experimental program was conducted in a glass walled tank, 90 ft. long, 2-1/2 ft. wide and 3 ft. deep at the Massachusetts Institute of Technology Hydrodynamics Laboratory. A piston type shallow water wave generator was used to generate the experimental waves. A steel frame to support the spheres in the rigidly restrained tests was located 40 ft. downstream from the wave generator. A model beach at a slope of 15 horizontal to 1 vertical occupying the last 35 ft. of the tank served as an energy dissipator, satisfactorily limiting undesirable wave reflections

The spheres were moulded from 1/4 inch lucite. Provision was made for attaching a 1/4 inch rod for the rigidly restrained tests and a mooring line for the moored tests.

In order to obtain a range of frequency ratios for each sphere in each test wave, the natural frequency of the sphere was varied by changing its weight. Filler materials were provided by mixing a commercially available dry detergent, Vermiculite, and granulated salt.

For the rigidly restrained tests the spheres were supported from the test stand as shown in Figure 6. The 3/4 inch support rod was shielded by 1 inch inside diameter lucite pipe to minimize tare forces on the rod.

INSTRUMENTATION

Instrumentation was required in the test program to measure wave characteristics, the horizontal and vertical force components in the rigidly restrained tests and the mooring line tension components in the moored tests. Because of the unsteady nature of the phenomenon, most data were taken electronically and recorded on a Sanborn Model 150 four channel direct writing oscillograph. The recorder was equipped with a timing marker which recorded one second pulses along one margin.

Wave profiles were measured using a capacitive type wave probe.

The horizontal force component on the rigidly restrained spheres was measured using a portal gauge. The gauge is sensitive to shear alone and therefore measures the horizontal force on the cantilever beam below it irrespective of the distance to the point of application of the force. The sensing element in the portal gauge is a Schaevitz L.V.D.T.

THE DYNAMICS OF A SUBMERGED MOORED SPHERE IN OSCILLATORY WAVES

The vertical force component on the rigidly restrained sphere was measured with a double diaphragm lift gauge using the same sensing element as the portal gauge.

In the moored tests, the horizontal and vertical components of mooring line tension were measured using a two component balance. The gauge consists of a horizontal outer force beam to measure the vertical component and a vertical inner force beam to measure the horizontal component. Both force beams have sensing elements consisting of 4 SR-4-A-7 strain gauges. Since the two component balance was used under water it was necessary to waterproof the strain gauges and wire connection. This was done by applying three or four coats of Neoprene Bonding Cement. Each coat was allowed to dry for 24 hours before the next was applied. The waterproofing successfully withstood continuous immersion for periods up to two weeks and intermittent immersion for a year.

RESULTS

RIGIDLY RESTRAINED TESTS

Experimental horizontal and vertical wave component histories for test I-2-A are presented in Figure 7. The experimental force traces show the inertial character of the wave forces of the test program as predicted by the low period parameters. The maxima of the horizontal component occur near 0° and 180° and the maxima of the vertical component near 270° and 90° . The horizontal component at 90° and 270° , the phase angles where the drag contribution to the total force is a maximum, is negligible.

From the experimental force histories, values of the inertia coefficient C_M , were determined for all tests. These values were determined to give the best fit between the experimental traces and the theoretical expressions given by equations (12) and (21). The inertia coefficients determined from the horizontal force component averaged 1.56 compared with the potential flow value of 1.50. The coefficients determined from the vertical component averaged 1.30.

From the experimentally determined inertia coefficients and equations (12) and (21) horizontal and vertical force component traces were computed for test I-2-A. For both traces the steady state value of C_D , 0.42 was used. The computed traces are shown as solid lines in Figure 7. The agreement with experiment is excellent.

PARTIALLY RESTRAINED TESTS

Mooring line forces and angles

The experimental mooring line dynamic horizontal and vertical tension component and mooring line angle histories for two tests are presented in Figures 8 and 9. The tests selected represent the extreme wave characteristics and period parameters of the test program. The mooring line tension components were obtained directly from the experimental records. The experimental mooring line angles were computed from the tension component traces using the relation

COASTAL ENGINEERING

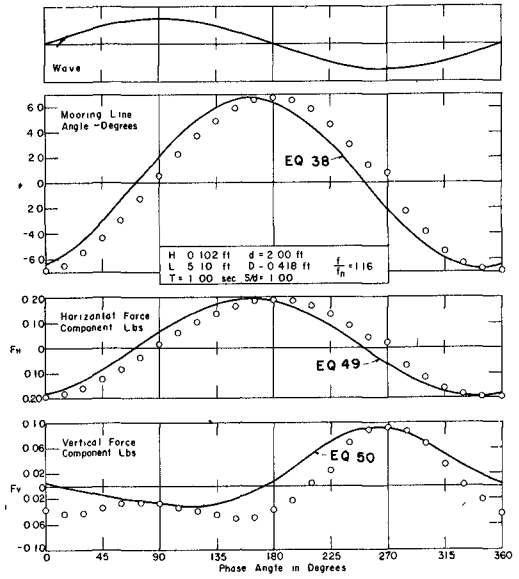
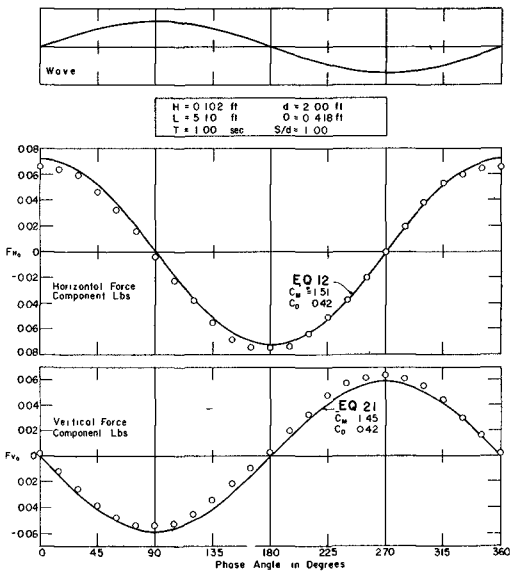


Fig. 7. Force component variation with wave phase - rigidly restrained sphere (test I-2-A).

Fig. 8. Force and mooring angle variation with wave phase (test I-2-A-2).

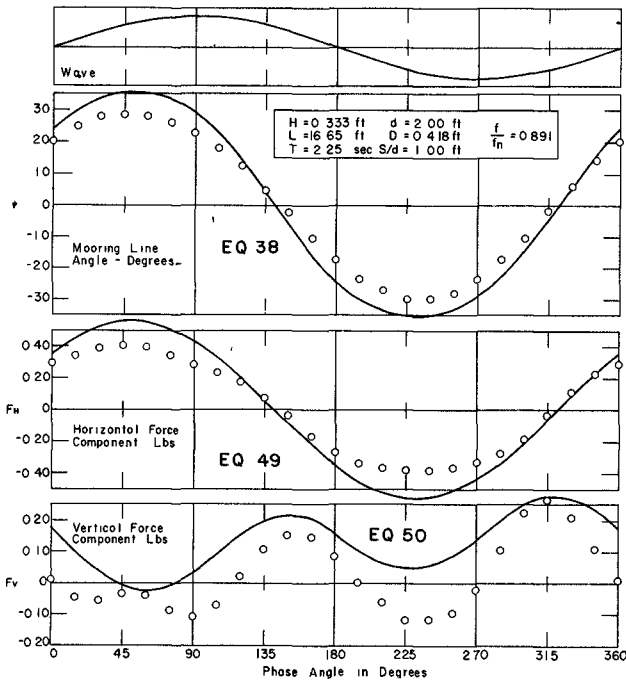


Fig. 9. Force and mooring angle variation with wave phase (test I-7-A-3).

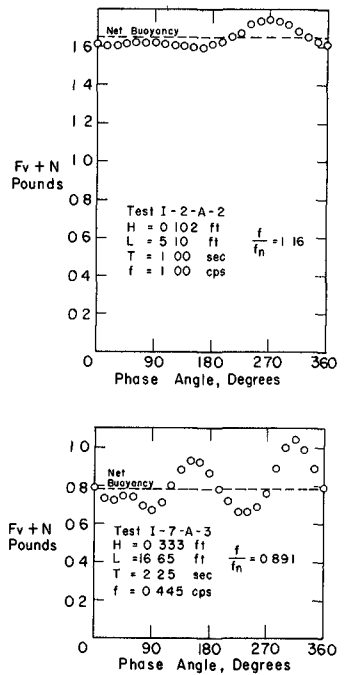


Fig. 10. Variation of vertical mooring force with wave phase.

THE DYNAMICS OF A SUBMERGED MOORED SPHERE
IN OSCILLATORY WAVES

$$\psi = \tan^{-1} \left(\frac{F_H}{F_V + N} \right) \quad (47)$$

For each experimental trace in Figures 8 and 9 a corresponding theoretical history was computed. The theoretical expression for the mooring line angle is given by equation (38).

In view of the assumptions made in the development of the theory, that the dynamic vertical force is much less than the net buoyancy and that the mooring line angle is small, the mooring line angle may be expressed

$$\psi = \frac{F_H}{N} \quad (48)$$

By substitution into equation (38), the theoretical horizontal force component history becomes

$$F_H = F_{H_m} \cos(\sigma t - \phi) \quad (49)$$

To solve for the theoretical mooring line angle and horizontal mooring force histories it is necessary to know F_{H_m} and the phase shift angle, ϕ . Equation (39) gives F_{H_m} in terms of the multiplication factor, $F_{H_m}/F_{H_{om}}$. The phase shift, ϕ , is given by equation (40). The multiplication factor and phase shift are functions of the frequency ratio and damping factor, n_2 . The damping factor, given by equation (43), is a function of the coefficients of inertia and drag and the maximum horizontal force component on the sphere in the rigidly restrained condition. In evaluating the theoretical horizontal force component and mooring line angle histories the following quantities were used:

- $C_M = 1.5$, potential flow value
- $C_D = 0.42$, steady state value
- $F_{H_{om}}$ = average of positive and negative experimental value in rigidly restrained tests

The agreement between the theoretical and experimental horizontal component and mooring line angle histories in Figures 8 and 9 is good with respect to curve shape and phasing. For the longer wave, I-7, the maxima of the theoretical curves are significantly higher than the experimental maxima representing a corresponding discrepancy between the theoretical and experimental multiplication factors. This tendency will be further substantiated with the presentation of the complete test results.

Part of the discrepancy is due to the fact that the first assumption in the development of the theory is not valid for the greater wave lengths. This is shown in Figure 10 where the total vertical mooring line tension component is plotted against wave phase angle for the two tests shown in Figures 8 and 9. The total vertical component is equal to the dynamic vertical plus the net buoyancy. For the test in wave I-2, the total vertical component is approximately equal to the net buoyancy and assumption 1 is valid. For wave I-7, the dynamic vertical component, F_y , is a significant proportion of the net buoyancy and assumption 1 is poor. The physical reason for the difference is twofold. First, a given frequency ratio entails a smaller net buoyancy in wave I-7 than in wave I-2. Second,

COASTAL ENGINEERING

the rigidly restrained vertical component is greater for the longer wave which results in a greater value of F_V .

The dynamic vertical mooring line tension component F_V has not been previously analyzed. In the theoretical development it was considered a second order effect. Physically, F_V results from the centrifugal force on the sphere caused by its motion in a circular arc. This force is given by Newton's second law with the mass term written to include the virtual mass effect.

$$F_C = [m + \frac{K\omega D^3}{6}]a_r$$

The term a_r is the radial acceleration.

$$a_r = \dot{\psi}^2 \ell$$

By differentiating equation (38), $\dot{\psi}$ is obtained.

$$\dot{\psi} = -\frac{2\pi}{T} \psi_m \sin(\theta - \phi) = -\dot{\psi}_m \sin(\theta - \phi)$$

Therefore,

$$F_C = [m + \frac{K\omega D^3}{6}] \dot{\psi}_m^2 \ell \sin^2(\theta - \phi) = F_{Cm} \sin^2(\theta - \phi)$$

In addition to the centrifugal force there is another contribution to F_V . This is seen by considering the case of small sphere motion, i.e., small ψ . In this case the sphere is nearly stationary and the vertical force acting upon it approaches the vertical force component on the stationary sphere F_{V_0} . The dynamic vertical mooring line component is, therefore, taken to be the linear superposition of the centrifugal force and the vertical force component on the stationary sphere.

$$F_V = F_C + F_{V_0} \quad (50)$$

This superposition is shown graphically in Figure 11 for a case where the phase shift angle, ϕ , is 180° and $F_{Cm} = 2F_{V_0m}$. The term F_{V_0} in Figure 11 approximates a negative sine wave as shown by equation (21). The resulting theoretical F_V history is non-symmetrical. The positive maximum value exceeds the negative. Curves computed from equation (50) are shown in Figures 8 and 9. The F_{V_0} values used in computing these curves were obtained from the experimental vertical component histories on the stationary sphere. The agreement with experiment is good with respect to curve shape and maximum positive values of F_V .

Force multiplication factors

For each sphere test made in this study, horizontal force multiplication factors were computed from the maximum experimental forces. The multiplication factors for the 0.418 ft. sphere in each test wave are plotted against frequency ratio in Figures 12 through 15. In each of the figures the experimental points define resonance curves of the form of Figure 4. It is important to note, however, that theoretically the

THE DYNAMICS OF A SUBMERGED MOORED SPHERE IN OSCILLATORY WAVES

experimental points of a particular test should not fall on a single curve of Figure 4 since these curves are drawn for constant values of the damping factor n_2 . For the conditions of the sphere tests the damping factor varies slightly with the frequency ratio.

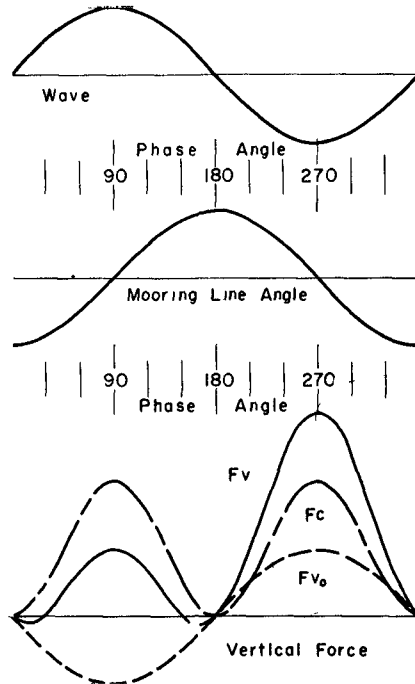


Fig. 11. Dynamic vertical mooring force by superposition.

For each set of experimental data in Figures 12 through 15 a theoretical curve is shown computed from equations (39) and (43). In all computations an inertia coefficient, $C_M = 1.5$ and a drag coefficient, $C_D = 0.42$ were used.

The agreement between theory and experiment is very good for short waves and becomes poorer as the wave length increases. One reason for the discrepancy between theory and experiment in the longer waves (involving the validity of the first assumption made in the development of the theory) has been discussed previously. Another possible cause of error is the value of C_D used in the computation of the theoretical curves. Because of the relatively small drag components encountered in this study it was not possible to determine C_D values from the rigidly restrained test data. The damping factor is shown by equation (43) to be proportional to C_D and the effect of the damping factor on the theoretical force multiplication factor is shown in Figure 4. It is seen that an increased damping factor would bring the theory into better agreement with experiment for the longer waves at frequency ratios less than about 1.4. For higher frequency ratios the damping coefficient has a small effect on the multiplication factor and the discrepancy would still persist. In any event more information would be needed such as would be obtained from a complete determination of the C_D vs. $u_m T/D$ curve before the use of a higher value of C_D could be justified.

COASTAL ENGINEERING

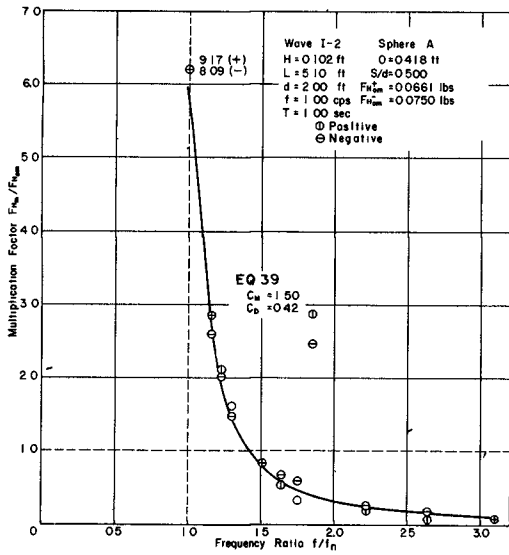


Fig. 12. Variation of horizontal mooring force with frequency ratio (test I-2-A).

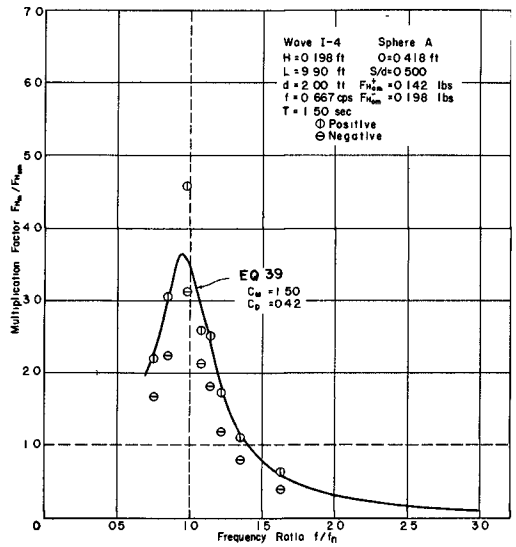


Fig. 13. Variation of horizontal mooring force with frequency ratio (test I-4-A).

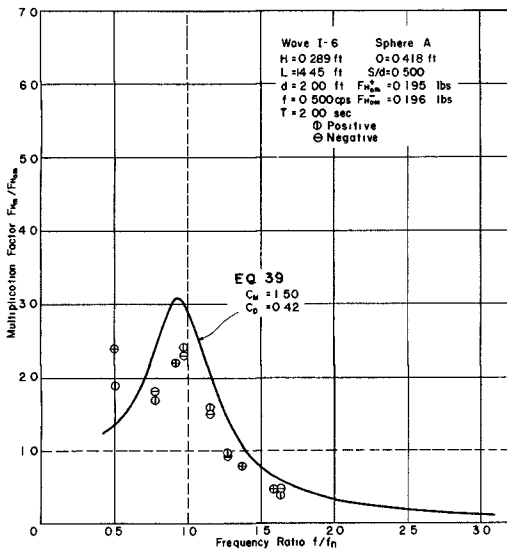


Fig. 14. Variation of horizontal mooring force with frequency ratio (test I-6-A).

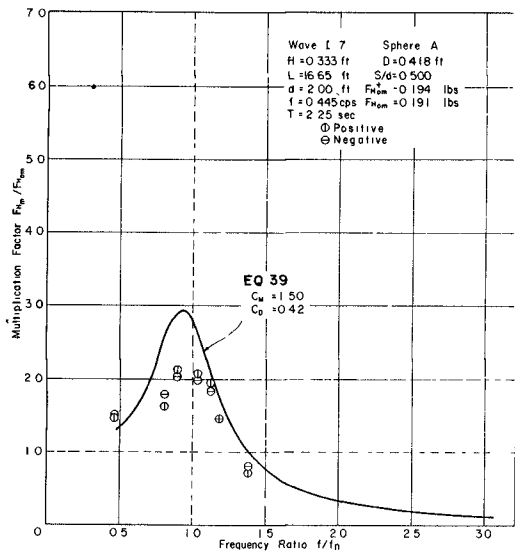


Fig. 15. Variation of horizontal mooring force with frequency ratio (test I-7-A).

THE DYNAMICS OF A SUBMERGED MOORED SPHERE IN OSCILLATORY WAVES

Two interesting features are noted in the test results. In Figure 14 the experimental points at $f/f_n = 0.5$ appear high. This is probably due to the fact that the waves have a second harmonic which is neglected in the Airy theory. Therefore, at f/f_n near 0.5, the system resonates with the second harmonic. In Figure 12 another high experimental point is seen; this one at $f/f_n = 1.85$. The phenomenon of a second resonance near $f/f_n = 2$ has been treated in mechanical vibration literature (Den Hartog, 1956) under the name "subharmonic resonance". There it is stated that the phenomenon may occur in a system having non-linear characteristics and that the analysis of the conditions under which subharmonic resonance will occur is extremely difficult. The mechanical system investigated in this study has non-linear damping and restoring force characteristics, the latter being assumed linear in the development of the theory. It is therefore possible that the observed second resonance is an inherent characteristic in the moored object problem. It is also possible that the second resonance could have been caused by reflected waves in the wave tank having a frequency equal to 1/2 the incident wave frequency. Extensive additional study would be necessary for the analysis of the second resonance phenomenon.

CONCLUSIONS

It is concluded that the behavior of moored submerged buoyant objects in oscillatory waves is adequately described by vibration theory with square law damping. The relationships presented herein accurately predict the mooring line tensions and motions of a sphere moored by a single vertical line when the following conditions assumed in the development of these relations obtain:

- 1) Predominant inertia force.
- 2) Small dynamic vertical mooring force with respect to net buoyancy.
- 3) Small maximum mooring line angle.
- 4) Small amplitude waves.

REFERENCES

- Den Hartog, J. P. (1956). Mechanical vibrations, fourth edition: McGraw-Hill Book Co. Inc.
- Dronkers, J. J. and Schonfeld, J. C. (1955). Tidal computations in shallow water: Proc. A.S.C.E. Sep. No. 714, Hyd. Div., June 1955.
- Harleman, D. R. F. and Shapiro, W. C. (1955). Experimental and analytical studies of wave forces on offshore structures, Part I, Results for vertical cylinders: M.I.T. Hydrodynamics Laboratory Technical Report No. 19.
- Jacobsen, L. S. (1930). Steady forced vibrations as influenced by damping: Trans. A.S.M.E., Vol. 52, No. APM 52-15.
- Keulegan, G. H. and Carpenter, L. H. (1956). Forces on cylinders and plates in an oscillating fluid: National Bureau of Standards Report 4821.